Kinetics of Excited States of Pigment Clusters in Solubilized Light-Harvesting Complex II: Photon Density-Dependent Fluorescence Yield and Transmittance

René Schödel,* Frank Hillmann,* Thorsten Schrötter,* Joachim Voigt,* Klaus-D. Irrgang,# and Gernot Renger#
*AG Molekulare Biophysik und Spektroskopie, Institut für Physik der Humboldt Universität zu Berlin, and #Max-Volmer-Institut für Biophysikalische Chemie und Biochemie, Technische Universität Berlin, Berlin, Germany

ABSTRACT Relative fluorescence yield, Φ_F, and transmittance, T, were measured in solubilized light-harvesting complex II (LHCII) as a function of photon density, I_p, of monochromatic 645-nm laser pulses (duration: ~2.5 ns). Special efforts were made in constructing an optical set-up that allows the accurate determination of the fluorescence from an area of constant I_p. $\Phi_F(I_p)$ starts to decline at $\approx 10^{14}$ and drops to values below 0.01% at maximum I_p ($\approx 10^{19}$ photons cm^{-2} $pulse^{-1}$). $T(I_p)$ decreases only slightly at photon densities of $\approx 10^{15}$ but increases steeply at values of $>10^{17}$ photons cm^{-2} $pulse^{-1}$. The interpretation of the $\Phi_F(I_p)$ data using the saturation limit of Mauzerall's multiple hit model leads to a unit size of about 10–15 chlorophyll molecules. One interpretation is to attribute this result to a very fast exciton-exciton annihilation of multiple excited states generated within this small domain. Alternatively, based on the assumption that delocalized cluster states within the monomeric/trimeric subunit of LHCII exist, the results can be consistently described by a kinetic model comprising ground, monoexcitonic, and biexcitonic states of clusters and a triplet state that is quenched by carotenoids in LHCII. Within the framework of this model the annihilation of multiple excitations is explained as ultrafast radiationless relaxation of higher excited cluster states. Comparative measurements in diluted acetonic Chl a solution are consistently described by the depletion of the ground state, taking the absorption cross section at the used wavelength.

INTRODUCTION

The photosynthetic transformation of solar radiation into Gibbs energy comprises three types of reaction sequences: 1) formation of electronically excited states and their radiationless transfer to the photochemically active pigment P within the reaction center, 2) electron transfer from the excited singlet state $^1P^*$ to an associated acceptor component A and subsequent stabilization of the primary charge separation by rapid electron transfer from A^- to further acceptor component(s), and 3) dark reactions of the oxidizing and reducing redox equivalents (for a review, see Renger, 1992).

To ensure efficient trapping of light and to permit optimal adaptation to different illumination conditions, photosynthetic organisms have developed suitable antenna systems consisting of pigment protein complexes. During the last decade significant progress has been achieved in the isolation and spectral characterization of individual pigment protein complexes that constitute antenna systems of photosynthetic organisms (Jansson, 1994; Thornber et al., 1994; Paulsen, 1995). Among them the trimeric light-harvesting complex II (LHCII) of green plants is one of the best characterized systems. It constitutes the major part of the photosystem II (PS II) antenna in green plants and accounts for about 50% of the total chlorophyll content of the thylakoid membrane (see Kühlbrandt, 1994). The LHCII has been resolved to 3.5 Å by electron crystallography of two-dimensional crystals (Kühlbrandt et al., 1994). Each subunit of the LHCII trimer was shown to bind at least 12 chlorophylls (seven Chl a, five Chl b) and two carotenoids. The chlorophylls are arranged in two layers, forming an upper and lower leaflet with respect to the plane of the thylakoid membrane (Kühlbrandt et al., 1994).

In spite of high trapping efficiencies of the reaction centers, loss processes of excited states are inevitable. One of them is the radiative emission (fluorescence) that provides an invaluable tool for monitoring the functional state of the photosynthetic apparatus, even in whole leaves (Renger and Schreiber, 1986). A wealth of information on the excited-state dynamics coupled with photosynthetic trapping in photosystem II (PS II) can be gathered from measurements of time-resolved fluorescence decay kinetics (for a recent review, see Holzwarth, 1989; Van Grondelle et al., 1994; and references therein).

Early measurements of the fluorescence yield of Chlorella as a function of excitation intensity using 7-ns pulses at 337 nm (Mauzerall, 1976a, 1978) showed a fivefold fluorescence yield decrease at the maximum intensity of about 10^{16} photon/cm^2 per pulse with respect to the low intensity limit. This decrease was not in accordance with the assumption of a "single hit" poisson saturation. Because of the "broad" character of the decrease, Mauzerall suggested that a second random process occurs if more than one photon is absorbed by a photosynthetic unit. Almost the same result for the decrease in the fluorescence yield was measured using 20-ps pulses (Campillo et al., 1976b). Therefore it was concluded that the curves of the fluorescence yield as a

Received for publication 12 March 1996 and in final form 29 August 1996.
Address reprint requests to Rene Schoedel, Institut für Physik der Humboldt Universität, Invalidstrasse 110, 10115 Berlin, Germany. Tel.: 49-30-2093-7668; Fax: 49-30-2093-7659; E-mail: schoedel@ physik.hu-berlin. de.

0006-3495/96/12/3370/11 $2.00

function of intensity are time independent for times shorter than 7 ns (Campillo et al., 1976b). As a consequence, triplets should play a minor role in this type of single-pulse experiment. The decrease in the fluorescence yield was attributed to singlet-singlet annihilation, i.e., a collision of two S_1 states leads to the formation of one ground state S_0 and a higher S_n state that undergoes a rapid radiationless decay to the state S_1. Based on this idea, several models were developed to describe the decline of the fluorescence yield. For systems consisting of sufficiently large pigment domains a description by continuous rate equations was proposed (Swenberg et al., 1976) as the limit of a more detailed model of master equations (Paillotin et al., 1979). Likewise, the acceleration of the fluorescence decay kinetics with increasing laser pulse intensity observed in chloroplasts (Seibert and Alfons, 1974; Paschenko et al., 1975; Beddard et al., 1975; Campillo et al., 1976a) could also be explained by singlet-singlet annihilation (for a review, see Breton and Geacintov, 1980). In most of the cases a very fast randomization of excitons within a domain was considered (Swenberg et al., 1976; Campillo et al., 1976a; Geacintov et al., 1977b; Paillotin et al., 1979). This assumption leads to a value for the singlet-singlet annihilation parameter that is independent of time and laser pulse intensity. Later a functional dependence of the singlet-singlet annihilation parameter on time and intensity was discussed (Rubin and Paschenko, 1986; Valkunas et al., 1995).

The annihilation of singlets by triplets was shown to dominate in the case where laser pulses of sufficiently large duration or multiple pulses were used for excitation (Breton and Geacintov, 1976; Geacintov et al., 1977a, 1978). A further master equation theory was developed by Paillotin et al. (1983a) that describes this singlet-triplet annihilation process. On the basis of this model, studies performed on a microsecond scale (Kolubajev et al., 1985) were used to determine the number of pigments that form a domain.

The above-mentioned results were all obtained for systems that contain a comparatively large number of coupled chlorophyll molecules, i.e., the excited singlet states can move during their lifetime over ensembles of about 2000–3000 pigments (Breton and Geacintov, 1980).

However, a markedly different feature is expected to arise in systems with a small number of strongly coupled chlorophyll molecules, e.g., in isolated (solubilized) LHCII subunits containing about seven Chl a and five Chl b. The center-to-center distances between the chlorophylls ranging from 9 to 14 Å within LHCII (Kühlbrandt et al., 1994) are comparable to the size of the chlorophyll molecule itself. In this densely packed pigment structure strong excitonic couplings between the pigments are expected (Van Grondelle et al., 1994). Low-temperature CD spectroscopy suggests a complicated set of excitonic interactions (Kwa et al., 1992). Even between pigments of different monomeric subunits, excitonic interaction arises (Nussberger et al., 1994). For such a system of strongly coupled chlorophylls, the excitonic wave functions are linear combinations of the wave functions of the individual pigments. The absorption of one photon by the pigment ensemble in the ground state leads to the first excited cluster state that is described by wave functions of the type

$$\sum_{i=1}^{Z} c_i \cdot \varphi_i^{ex} \cdot \prod_{\substack{j \\ j \neq i}}^{Z} \varphi_j,$$

where φ_i^{ex} is the wave function of the first excited state of a monomeric pigment i and φ_j describes the ground state of pigment j. The c_i coefficients are time independent for the case of stationary conditions, and Z is the number of pigments within the cluster. It must be emphasized that the first excited cluster state contains several individual exciton states. The excitation energy transfer within a cluster state is equivalent to relaxation between different exciton states of the ensemble of strongly coupled chlorophylls (Van Grondelle et al., 1994). The present study does not address this type of relaxation between different exciton states within the same cluster state. A different situation arises if a photon hits a pigment ensemble that has already attained the first excited cluster state. In this case absorption leads to a doubly excited cluster state described by a wave function of the type

$$\sum_{k,l} c_{k,l} \varphi_k^{ex} \varphi_l^{ex} \prod_{\substack{m \\ m \neq k,l}}^{Z} \varphi_m.$$

To our knowledge there have been only a few studies that have investigated the dependence of the fluorescence decay on the excitation intensity in solubilized forms of LHCII. Nordlund and Knox (1981), using laser pulses of 20 ps duration and 530 nm excitation wavelength, found that the fluorescence decay kinetic is virtually independent of the photon density up to values of 3×10^{18} photons/cm^2 per pulse. Two alternative explanations of this observation were offered (Nordlund and Knox, 1981): 1) very fast exciton-exciton annihilation during the 20-ps pulse corresponding to the Mauzerall limit (Mauzerall, 1976a) and 2) assumption of delocalized states within CPII comprising excited-state absorption and rapid radiationless decay of the delocalized higher excited state. The former idea was elaborated by Gülen et al. (1986), who described the fluorescence kinetics at high photon density in complexes with a small number of chromophors.

On the other hand, Rubin and Paschenko (1986), using 530-nm pulses of 6 ps duration found that the lifetime of their LHCP preparation decreased at intensities exceeding 10^{12} photons/cm^2 per pulse. This intensity corresponds to an average hit rate of one photon per at least 10,000 chlorophylls, and therefore these data probably reflect collisional excited state decay via a diffusion-limited process within a rather large domain.

In the present study we made measurements of the absorption and fluorescence emission of LHCII, as well as comparative measurements in diluted acetonic (80%) Chl a

solution as a function of the photon density of excitation laser pulses of about 2.5 ns duration. In the case of fluorescence measurements, particular emphasis was placed on achieving a sufficiently high spatial separation of the fluorescence emitted from the sample to avoid the effects of spatial nonuniformity (Paillotin et al., 1983b). The data reported were measured by using a special optical device.

MATERIALS AND METHODS

Sample material

PS II membrane fragments were isolated according to the method of Berthold et al. (Berthold et al., 1981, with some modifications as outlined in Völker et al., 1985). The isolation of LHCII was performed in the presence of β-dodecylmaltoside, as described in detail (Irrgang et al., 1988). The LHCII preparations were characterized by room temperature absorption spectroscopy using a Shimadzu UV 3000 spectrophotometer. Absorption maxima in the red were localized at 652 ± 1 and 675 ± 1 nm. Pigment concentration and Chl a/b ratio were determined by using the method of Porra et al. (1989). The latter value was found to be 1.35 ± 0.05. The polypeptide composition of the LHCII preparation has been checked by sodium dodecyl sulfate/urea/polyacrylamide gel electrophoresis using the method described by Irrgang et al. (1988). The LHCII preparation was diluted with a buffer containing 30 mM 2-(*N*-morpholino)ethanesulfonic acid-NaOH (pH 6.5), 10 mM $CaCl_2$, 20% w/v sucrose, and 0.025% w/v β-dodecylmaltoside. The total chlorophyll concentration of the sample was 0.20 mg Chl/cm^3.

The (ground state) absorption cross section σ at 645 nm of the LHCII samples related to single absorbing chlorophylls was estimated from the total Chl a/b concentration and the absorption spectrum of the LHCII samples analyzed in this study. In the case of small particle size, any contribution due to the flattening effect (Pulles et al., 1976) can be ignored and σ can be directly determined from the absorption data by the relation

$$\sigma(\lambda) = \frac{\alpha}{N^{\text{Chl-sample}}} = \frac{M_{\text{Chl}} \times \text{OD}(\lambda) \times \log(10)}{C_{\text{Chl}} \times N_A \times d}. \quad (1)$$

$N^{\text{Chl-sample}}$ is the total number of Chl a and Chl b molecules per cm^3 of the macroscopic sample (which, of course, is different from the concentration within the protein in LHCII), M_{Chl} is the molar mass (an average of 900 g/mol was used; exact values: $M_{\text{Chl a}}$ = 893.5 g/mol, $M_{\text{chl b}}$ = 907.5 g/mol), c_{Chl} is the total concentration of chlorophyll within the sample in units of mg/cm^3, N_A is Avogadro's number, OD(λ) is the optical density at λ, and d is the optical path length. At a 0.1-cm pathlength, the optical density at 645 nm was about 0.44 (≈ 36% transmittance). From Eq. 1 one obtains for the average optical cross section of a single absorbing chlorophyll within the LHCII at 645 nm, σ(645 nm) ≈ 0.75 × 10^{-16} cm^2.

Commercially available Chl a from spinach (Sigma Chemical Co.) was dissolved in a mixture of 80% v/v acetone (Roth GmbH and Co., high-performance liquid chromatography grade). The concentration was about 0.2 mg Chl/cm^3 (≈ 0.22 mM). According to Porra et al. (1989), the decadic extinction coefficient ε of Chl a in acetonic solution at 646.6 nm is 18,580 M^{-1} cm^{-1}. Therefore, the absorption cross section at this wavelength is obtained by using the relation $\sigma = \epsilon \times \log(10)/N_A$ (N_A is Avogadro's number), which results in $\sigma_{\text{Chl a}}$(646.6 nm) = 0.71 × 10^{-16} cm^2. The absorption cross section at the wavelength used in this study can be estimated by using the ratio of the optical densities OD(646.6 nm)/OD(645 nm). The result is $\sigma_{\text{Chl a}}$(645 nm) = 0.63 × 10^{-16} cm^2.

Experimental set-up and measuring conditions

Fluorescence measurements

The samples were excited with repetitive (10 Hz), highly monochromatic ($\Delta\lambda \approx 0.002$ nm) 645-nm pulses from a Nd^{3+}-YAG-laser pumped dye laser (LAS LDL 105). The maximum pulse energy applied was 500 μJ.

A system of three wheels, each containing four calibrated neutral density filters, was used to adjust the photon density of the pulses impinging on the sample. The laser beam was focused by an objective of 14 cm focal length. The dimension of the spot within the focal plane was about 20 μm. To minimize the influence of beam displacement caused by the neutral density filters, the sample was positioned outside of the focus. The measurements were performed using various spot sizes measured with a 5-μm pinhole, which was moved in two dimensions by step motor-driven translation elements (the spot was imaged in an analogous way by Kolubajev et al., 1985). The smallest spot used was about 60 μm in diameter. In this way a very high excitation photon density of about 10^{19} photons/cm^2 per pulse could be achieved.

The optical path length of the cuvette was 0.2 mm to minimize effects due to inhomogenous sample illumination. A second objective of 14 cm focal length was used to display the fluorescence-emitting area through a pinhole (Fig. 1). The angle of the optical axis of this projection was <10°, and the magnification factor was about 2.5. An appropriate size of the pinhole permitted the selection of the fluorescence emitted only from the region of highest excitation (around the center) and almost constant photon density, which varied by no more than 30%. Emissions from areas excited with fewer photons were suppressed. A set of pinholes was available for adaptation to the spot size used. This device ensured that the fluorescence signal was related to a well-defined photon density of excitation. The maximum photon density in the center of the spot was precisely determined from spot data and pulse energy.

After passing a monofiber illuminator, the fluorescence signal was coupled to a double monochromator (Carl Zeiss Jena; GDM 1000). The measurements were performed at a fluorescence wavelength of 680 nm. A highly sensitive avalanche diode amplifier module (Analog Modules; type 712-A4) was used as a detector. The signal, corresponding to the fluorescence, together with a reference signal of the excitation beam, was transferred into a boxcar integrator that was operating in the gate mode (gate width 40 ns). The analog signals obtained were digitized (Advantech and Co.; PCL 812 card) and stored on a hard disk. The relative fluorescence yield was calculated from the normalized ratio of emission and excitation intensity. The time course of excitation was measured with a fast microchannel multiplier and a high-frequency oscilloscope (Tektronix 684A), which allowed us to observe single pulses, which can be approximately described by a Gaussian profile. Thus the time course of the photon density $I(t)$ (in units of photons/cm^2/s) is given by

$$I(t) = I_p \frac{1}{\Delta \cdot \sqrt{2\Pi}} \cdot \exp\left[\frac{(t - t_0)^2}{2 \cdot \Delta^2}\right]. \quad (2)$$

I_p is the integral photon density per pulse, Δ = 1.1 ns (Gaussian width), and t_0 is the time at which the pulse reaches its temporal maximum. This

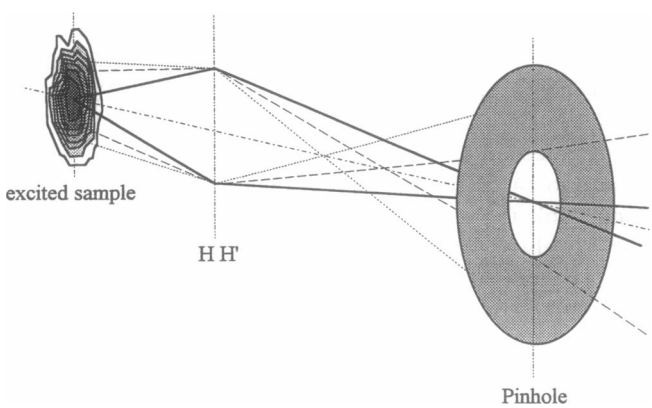

FIGURE 1 Schematic description of selective scanning of fluorescence emission from the highly excited area. Fluorescence beams (*dashed lines*) emitted from low excited regions cannot pass the pinhole.

excitation pulse duration of ~2.5 ns (FWHM) is short enough to avoid a considerable population of triplet states during the pulse (Campillo et al., 1976b). Furthermore, the low repetition rate of 10 Hz permits a complete decay of triplets during the dark time between the pulses.

Transmittance experiments

The same laser pulses as in the fluorescence measurements were used to investigate the photon density-dependent transmittance of LHCII. After passing a sample cuvette of 1 mm optical pathlength and subsequent compensation by additional density filters, the transmitted photons reached a detector (Analog Modules; type 712-A2). The further signal processing was the same as described under Fluorescence measurements, above. The value of the transmittance was calculated for each pulse from the ratio of transmitted and hitting photons (reference signal). The data were adjusted to the case of low photon densities (optical linear case) known from OD(λ = 645 nm).

Kinetic model for Chl a and delocalized exciton states within solubilized LHC II

This proposed model describes the ground-state depletion of diluted Chl a in 80% acetonic solution (in this case the triplet transfer to carotenoids must be left out) and permits the calculation of the population of excited cluster states within solubilized LHCII units under the assumption that there is no interaction between them. This condition can be satisfied in the case of states delocalized within a solubilized LHC II unit, whereas the interaction of excited states between different solubilized trimeric subunits can be neglected.

The description comprises six states of the cluster: ground state, first and second excited singlet states, a triplet state, and a carotenoid singlet ground and triplet state, respectively. The following processes are taken into account: ground- and excited-state absorption, decays of excited states, intersystem crossing to the Chl triplet state, and decay and the quenching of Chl triplets by carotenoids and their decay. This model, illustrated in Fig. 2, leads to the following system of six coupled differential equations:

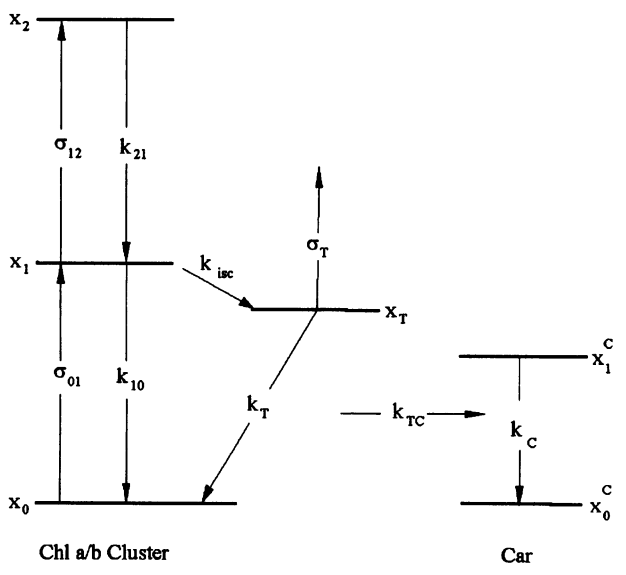

FIGURE 2 Illustration of pathways (see text) leading to the population of (first and second) singlet-excited states x_i (Chl a/b) as well as the intersystem crossing into a triplet state. In LHCII the triplets are quenched by carotenoids.

$$\frac{d}{dt}x_0(t) = -\sigma_{01}\cdot I(t)\cdot x_0(t) + k_{10}\cdot x_1(t) + k_T\cdot x_T(t) + k_{TC}\cdot x_T(t)\cdot x_0^C(t) \quad (3a)$$

$$\frac{d}{dt}x_1(t) = +\sigma_{01}\cdot I(t)\cdot x_0(t) - \{k_{10} + k_{isc} + \sigma_{12}\cdot I(t)\}\cdot x_1(t) + k_{21}\cdot x_2(t) \quad (3b)$$

$$\frac{d}{dt}x_2(t) = \sigma_{12}\cdot I(t)\cdot x_1(t) - k_{21}\cdot x_2(t) \quad (3c)$$

$$\frac{d}{dt}x_T(t) = k_{isc}\cdot x_1(t) - k_T\cdot x_T(t) - k_{TC}\cdot x_T(t)\cdot x_0^C(t) \quad (3d)$$

$$\frac{d}{dt}x_1^C(t) = -k_C\cdot x_1^C(t) + N/N_C\cdot k_{TC}\cdot x_T(t)\cdot x_0^C(t) \quad (3e)$$

$$\frac{d}{dt}x_0^C(t) = +k_C\cdot x_1^C(t) - N/N_C\cdot k_{TC}\cdot x_T(t)\cdot x_0^C(t), \quad (3f)$$

where x_i (i = 0, 1, 2, T) represents the populations of the states normalized to the total concentration N (i.e. $x_i = n_i/N$), and x_1^C and x_0^C are the relative populations of carotenoid triplet and ground states, respectively ($x_{0/1}^C = n_{0/1}^C/N_C$, N_C = total carotenoid concentration).

σ_{01} and σ_{12} are the absorption cross sections of ground and first excited states, k_{10} and k_{21} are the rate constants of the monomolecular relaxation channels, and k_{isc} is the rate constant of intersystem crossing. k_{TC} is the transfer rate from chlorophyll triplets to carotenoid triplets, and k_T and k_C are the decay rates of these populations. $I(t)$ is the photon density of the pulses that is described by Eq. 2. Some of the parameters are known from the literature; the others are running free for the numerical fit of the experimental data (see Results). Equations 3a and 3f are not required because they are linearly dependent on the other ones. Because the total number of chlorophyll and carotenoid states remains constant, the populations of the ground states x_0 and x_0^C are given by $x_o(t) = 1 - x_1(t) - x_2(t) - x_T(t)$ and $x_0^C = 1 - x_1^C$, respectively.

Terms for stimulated emission are not considered for the following reason. At the excitation wavelength (λ = 645 nm, highly monochromatic: $\Delta\lambda \approx 0.002$ nm) the population of resonant states is rather small, owing to rapid redistribution among inhomogeneously broadened states and transfer to wavelengths at which fluorescence takes place (the fluorescence at 645 nm is negligibly small).

As the fluorescence emission is assumed to originate only from the first excited state(s), the following expression is obtained for the relative fluorescence yield $\Phi_F(I_p)$:

$$\Phi_F(I_p) = \frac{\int_{-\infty}^{\infty} x_1(t)\cdot dt}{I_p} \Big/ \left[\frac{\int_{-\infty}^{\infty} x_1(t)\cdot dt}{I_p}\right]_{I_p\to 0}. \quad (4)$$

The numerical value of the transmittance $T(I_p)$ that corresponds to the measured integral transmittance by integration over the time-dependent "transmitted" photon density $I_{Trans}(t)$ is

$$T(I_p) = \frac{1}{I_p}\int_{-\infty}^{\infty} I_{Trans}(t)\cdot dt. \quad (5)$$

For the first simplest case $I_{Trans}(t)$ is obtained by taking Beer's law: $I_{Trans}(t) = I(t)\cdot\exp[-\alpha(t)\cdot d]$, where $\alpha(t)$ is the time-dependent absorption coefficient and d is the optical path length. However, α is also a function

of photon density that additionally varies as a function of optical pathway (about 36%) within the sample. Therefore, $\alpha(I,t)$ is used to solve the differential equation for the decrease in photon density within the sample (see below).

$\alpha(I, t)$ was gathered from $\alpha(I, t) = N^{\text{sample}} \cdot \{\sigma_{01} \cdot x_0(I, t) + \sigma_{12} \cdot x_1(I, t) + \sigma_T \cdot x_T(I, t)\}$, where the additional absorption cross section σ_T is responsible for chlorophyll triplet state absorption (a contribution of carotenoids to the 645 nm absorption can be neglected; for a review, see Siefermann-Harms, 1987). N^{sample} is the macroscopic (average) concentration within the sample. In dilute Chl a solution N^{sample} is the number of Chl a per cm^3. In the case of solubilized LHCII N^{sample} represents the average cluster concentration resulting from α^0/σ_{01}, where α^0 is the linear absorption coefficient obtained from the optical density OD at a given pathlength d ($\alpha^0 = \log(10) \cdot \text{OD}/d$), and σ_{01} is the ground-state absorption cross section of the clusters.

To account for the decrease in $I(y, t)$ (in the case of nonlinear absorption at higher pulse intensity), the numerical solution (Eqs. 3b–3e) was performed in the following way. The time course of the pulse was separated into k time intervals $\{t_j, t_j + 1\}$ that are short with respect to the overall pulse duration but long compared with the passage time of the light through the sample (about 3 ps). At first, $\alpha(I(t_j))$ was calculated for all times t_j and for various intensities I, and then a continuous function $\alpha(I(t_j))$ of I was generated by interpolation. For each time interval the decrease of $I(y, t_j)$ is given by

$$\frac{d}{dy} I(y, t_j) = -\alpha(I(y, t_j)) \cdot I(y, t_j). \quad (6)$$

This is the differential equation for the decrease in the initial intensity $I(0, t_j)$ (known from Eq. 2) to $I(d, t_j)$ at $y = d$. The total pulse intensity that passed the sample is given by $\sum_j^k I(d, t_j) \cdot (t_j - t_{j-1})$. A normalization to the total pulse intensity at $y = 0$ gives the overall transmittance $T(I_p)$ that is experimentally determined:

$$T(I_p) \cong \frac{\sum_j^k I(d, t_j) \cdot (t_j - t_{j-1})}{\sum_j^k I(0, t_j) \cdot (t_j - t_{j-1})} \cong \frac{1}{I_p} \cdot \sum_j^k I(d, t_j) \cdot (t_j - t_{j-1}). \quad (7)$$

All calculations where carried out using Mathematica v.2.2 (Wolfram Research).

RESULTS

Experimental data

Fig. 3 illustrates that a careful spatial selection of photons emitted from a homogeneously illuminated sample area is the indispensable prerequisite for obtaining reliable results that deserve further analysis. Drastic deviations can be observed among the shapes of the $\Phi_F(I_p)$ curves measured at different spatial selectivities of fluorescence emission. In the case of insufficient separation the $\Phi_F(I_p)$ curves exhibit a markedly less pronounced decline. This finding is consistent with the theoretical considerations of Paillotin et al. (1983b).

Fig. 4 shows the curves measured in solubilized LHCII and in 80% v/v acetonic solutions of Chl a. The measurements cover a range of almost four decades of the relative fluorescence yield and five decades of photon density. An inspection of these data readily reveals a striking feature: the shape of the curve $\Phi_F(I_p)$ is virtually the same for solubilized LHCII and Chl a in acetone, but in the former sample the curve is shifted by about 1.1 logarithmic units

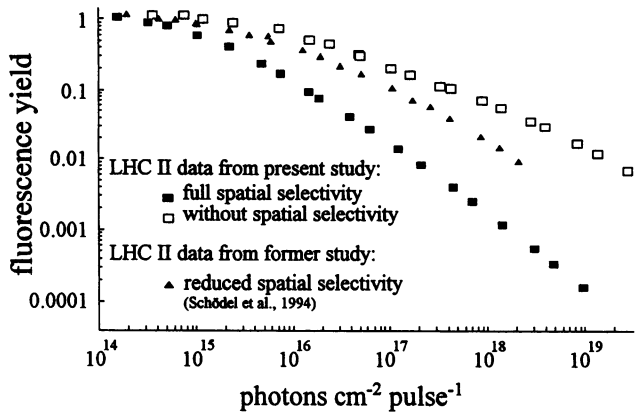

FIGURE 3 Normalized fluorescence yield of LHCII complexes resulting from measurements with different spatial selectivity in detecting the fluorescence signal as a function of photon density.

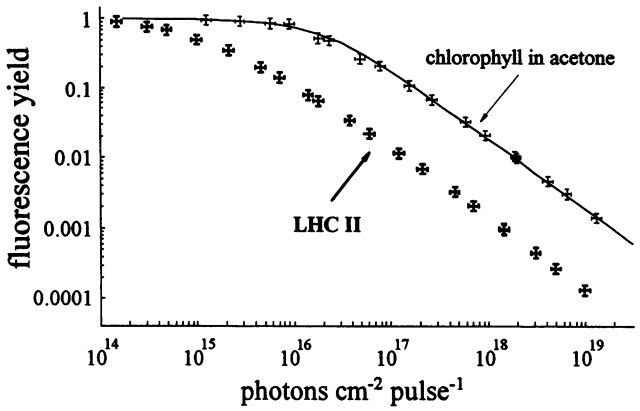

FIGURE 4 Normalized fluorescence yield as a function of the photon density in solubilized LHCII complexes and solution of Chl a in (80% v/v) acetone measured under conditions of high spatial selectivity. The solid line for Chl a is calculated (see text) with the following parameters: $\sigma_{01}(645\text{ nm}) = 0.62 \cdot 10^{-16}\ cm^2$, $k_{10} + k_{isc} = 1/(5.5\text{ ns})$, $k_{isc} \approx 1/(7\text{ ns})$, $k_{21} > 1/(100\text{ ps})$, $k_{TC} = 0$, $k_T = 1/(400\ \mu s)$.

toward lower values of I_p. A shift of $\Phi_F(I_p)$ curves was also found by Geacintov et al. (1979) when comparing measurements performed with 10-ns pulses (wavelength 337 nm) in Chl a solution and chloroplasts. However, these data are not directly comparable because the exciton dynamics are expected to be significantly different in chloroplasts and solubilized LHCII. In addition, the range of $\Phi_F(I_p)$ and I_p is much wider in the present study.

For further characterization of the optical properties of solubilized LHCII, the transmittance was monitored under the same excitation conditions as those used in the fluorescence measurements. The results obtained are depicted in Figs. 5 and 6. They show that at $I_p > 10^{15}$ photons cm^{-2} $pulse^{-1}$, the transmittance starts to decline, reaching a minimum value of about 10% decrease at around 10^{17} photons cm^{-2} $pulse^{-1}$ followed by a steep increase above 10^{18} photons cm^{-2} $pulse^{-1}$.

In contrast to the drastic decrease in the fluorescence yield to 0.01%, the spectral distributions of the fluorescence

of LHCII and Chl a are independent of the photon density of the pump pulses (data not shown). This finding is the experimental basis for the assumption that there are no additional radiative pathways contributing to the fluorescence at 680 nm at higher excitation photon densities. Furthermore, there seems to be no influence of the electric field that corresponds to the excitation intensity.

To exclude possible effects owing to irreversible changes of the sample during the measurements, repeated "forward-backward" check experiments were performed. In the forward case the measurements were started at a minimum photon density that was subsequently increased, whereas in the opposite direction (i.e., the backward case), the same measurements were started at the highest photon density. No difference was observed. Furthermore, the fluorescence spectra monitored before and after the measurements were virtually the same. Likewise, a dislocation of the sample from spot to spot (without changing the geometry) did not influence the data. Therefore, there is no indication of effects originating from irreversible sample modification during the course of the measurements.

Fits to the data

Chl a in solution

In the case of low Chl a concentrations in 80% v/v acetonic solution, a bimolecular excited state annihilation can be ignored. Furthermore, quenching of Chl a triplets by carotenoids does not exist ($k_{TC} = 0$). Based on the latest measurements (Vasilev et al., 1996), a lifetime of 5.5 ns was used for Chl a in solution. The intersystem crossing rate k_{isc} is about 1/(7 ns) (Bowers and Porter, 1967). Furthermore, a rapid ($k_{21} > 1/100$ ps) internal conversion of higher excited singlets was taken into account. With these values and an absorption cross section value σ_{01} of 0.62×10^{-16} cm^2 that is virtually the same as that gathered from the decadic extinction coefficient (see Materials and Methods), the experimental curve can be perfectly fitted with the proposed kinetic model (vide supra). Accordingly, the decline in the normalized fluorescence yield of Chl a in diluted solution at increasing I_p can be ascribed to ground-state depletion of noninteracting Chl a molecules, as shown in Fig. 4.

Solubilized LHCII

The fluorescence yield of solubilized LHCII exhibits a decline that is similar in shape to that of Chl a in dilute solution, but the curve is markedly shifted toward lower photon densities, i.e., Φ starts to decline at values exceeding 10^{14} photons cm^{-2} pulse^{-1} (see Fig. 4). In an attempt to fit this curve, the case of the "Poisson saturation limit" discussed by Mauzerall (1976a,b) was analyzed. Within the framework of this idea it is assumed that there are units, each consisting of ν chlorophyll molecules, and that the fluorescence response of each unit is the same for $\kappa \geq 1$ hit(s) per unit. The probability $p(\nu, \kappa, \pi)$ of hitting κ of the ν chlorophylls depends on the mean hit rate π of each of the chlorophyll molecules of the total ensemble and is given by the binomial distribution

$$p(\nu, \kappa, \pi) = \binom{\nu}{\kappa} \cdot \pi^{\kappa} \cdot (1 - \pi)^{\nu - \kappa},$$

The mean hit rate per chlorophyll is given by $\sigma \times I_p$, where the chlorophyll-related ground-state absorption cross section was determined to be 0.75×10^{-16} cm^2 (see Materials and Methods). At very high I_p values there are multiple hits per chlorophyll. This would give rise to higher excited states of individual chlorophyll molecules that rapidly relax to the lowest excited singlet state (ps time domain). Therefore, this effect will be not considered explicitly, and π is set to 1 for $\sigma \times I_p \geq 1$. Based on the above-mentioned assumption that the fluorescence is the same for each value $\kappa \geq 1$, the fluorescence yield is given by

$$\Phi \propto \frac{1}{\upsilon \cdot \pi} \cdot \sum_{\kappa=1}^{\upsilon} p(\upsilon, \kappa, \pi) = \frac{1 - p(\upsilon, 0, \pi)}{\upsilon \cdot \pi} = \frac{B(\sigma \cdot I_p)}{\upsilon \cdot \sigma \cdot I_p}, \tag{8}$$

where

$$B(\sigma \cdot I_p) = \begin{cases} 1 - (1 - \sigma \cdot I_p)^{\upsilon}, & \text{if } \sigma \cdot I_p < 1 \\ 1, & \text{else} \end{cases}$$

For large ν and $\pi = \sigma \times I_p \ll 1$, the binomial distribution is approximately given by a Poisson distribution around $\nu \times \sigma \times I_p = \sigma_{unit} \times I_p$ (average hit rate per unit), which leads to

$$\Phi \propto \frac{1 - e^{-\sigma_{unit} \cdot I_p}}{\sigma_{unit} \cdot I_p},$$

which is called the "Poisson saturation limit" (Mauzerall, 1976a,b).

Fig. 5 shows the measured data for the fluorescence yield

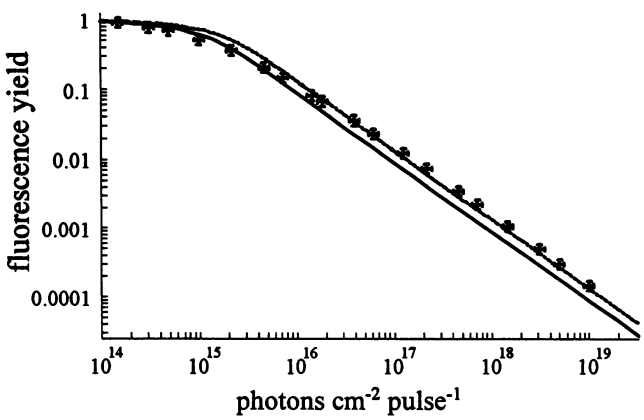

FIGURE 5 Normalized fluorescence yield as a function of the photon density in solubilized LHCII. The curves were calculated from Eq. 8 for a "multiple hit" model. The number of Chl a molecules within the unit was set to 15 (——) and 10 (– – –), respectively.

together with curves calculated with Eq. 8 for two different numbers ν of chlorophylls per unit. Taking $\nu = 15$, the data points at low I_p values are well described. On the other hand, the overall data set is better described with $\nu = 10$. Based on this analysis, the assumption seems to be confirmed that a second hit of a unit of LHCII consisting of 10–15 chlorophylls does not contribute to a radiative decay. This number ν corresponds to the experimentally determined chlorophyll content of a monomeric subunit of LHCII, i.e., a second hit during the pulse does not give rise to fluorescence emission. However, this finding does not provide any explanation for the "instantaneous" dissipation of all hits exceeding $\kappa = 1$. One possible explanation can be offered by the assumption of a very fast, collision-like mutual annihilation of diffusing excitons if more than one excited state is generated per unit (exciton-exciton annihilation). On the other hand, a closer inspection of the pigment array within LHCII leads to the idea of an alternative origin of rapid excited-state dissipation that takes place in the subunits.

Distances of 9–14 Å between the chlorophyll molecules (Kühlbrandt et al., 1994) are too short to satisfy the point dipole approximation used for calculations of the pairwise excited-state transfer according to Förster (1948). Furthermore, the interaction between the pigments is so strong (owing to the short intermolecular distances) that the transfer rate of excited states becomes comparable with vibrational and relaxation rates. In this case the exciton energy transfer of the pigment array cannot be described by a random walk of "localized" excited states with Förster rate constants for the pairwise transfer steps, as recently discussed by Mukamel and Rupasov (1995). Therefore, it seems to be more realistic to describe the excited-state dynamics within the subunit of solubilized LHCII by the assumption that absorption of photons by the pigment array gives rise to excitons that are delocalized. Within the framework of this model a hit by one photon leads to formation of the first excited cluster state (delocalized among the strongly interacting pigments of the unit). Accordingly, if a second photon is absorbed, this array is transferred into the second excited cluster state. It appears reasonable to assume that higher excited cluster states rapidly relax to the first excited cluster state and fluorescence is emitted from the latter state. The concept of delocalized excitons implies that the optical cross section σ of the cluster exceeds that of monomeric Chl (in the case of a simple linear aggregate the oscillator strength is proportional to the number of strongly coupled pigments; for a review, see Mukamel, 1995). Therefore, regardless of the detailed pigment array, the absorption cross section of a LHCII subunit is expected to depend on the number of chlorophylls in the pigment cluster. To account for this effect, the value of σ_{01} was used as a free running parameter of the data fit by the proposed kinetic model.

The fit procedure of the whole data set was performed in two steps. In comparison with the transmittance curves $T(I_p)$, the numerical fit of the fluorescence yield curves

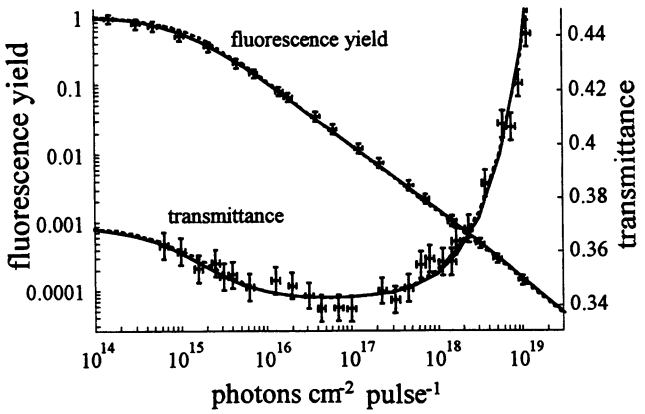

FIGURE 6 Normalized fluorescence yield and transmittance as a function of photon density in solubilized LHCII and calculated curves using: $k_{10} + k_{isc} = 1/(4.3\text{ ns})$, $k_T = 1/(400\ \mu s)$, $k_C = 1/(10\ \mu s)$, $k_{TC} = 1/(9\text{ ns})$ and $\sigma_{01}(645\text{ nm}) = 1.15 \cdot 10^{-15}\text{ cm}^2$, $k_{isc} \approx 1/(7\text{ ns})$, $k_{21} = 1/(0.25\text{ ps})$ (– – –) and $\sigma_{01}(645\text{ nm}) = 1.7 \cdot 10^{-15}\text{ cm}^2$, $k_{isc} \approx 0$, $k_{21} = 1/(0.1\text{ ps})$ (——), respectively. In both cases we set $\sigma_{12}(645\text{ nm}) = \sigma_T(645\text{ nm}) = 1.08 \cdot \sigma_{01}(645\text{ nm})$.

$\Phi_F(I_p)$ can be significantly simplified by the reasonable assumption of a fast decay channel of x_2 with $k_{21} > 1/(100$ ps). In this case only a small depletion of the x_1 population takes place, i.e., $\Phi_F(I_p)$ is marginally affected by σ_{12}. Likewise, σ_T can be ignored for a numerical fit of $\Phi_F(I_p)$. Therefore, at first the $\Phi_F(I_p)$ curves were fitted to obtain the parameter σ_{01}. In a subsequent step this value was used for the numerical fit of $T(I_p)$ that permits the extraction of the values for k_{21}, σ_{12}, and σ_T.

The lifetime of solubilized LHCII was set at 4.3 ns (Liu et al., 1993), and the triplet-triplet transfer rate constant k_{TC} is about 1/(9 ns) (Kramer and Mathis, 1980). The rate constants for ^{3}Chl and ^{3}Car decay are also taken from the literature: $k_T = 1/(0.4\text{ ms})$ (Siefermann-Harms, 1987) and $k_C = 1/(10\ \mu s)$ (Petermann et al., 1995). The intersystem crossing rate k_{isc} was varied between zero and 1/(7 ns).

Setting k_{isc} at zero, the best fit for the $\Phi_F(I_p)$ data is obtained with $\sigma_{01}(645\text{ nm}) = (1.7 \pm 0.1) \times 10^{-15}\text{ cm}^2$. Taking these values $T(I_p)$ can be satisfactorily fitted with $k_{21} = 1/(100$ fs) and $\sigma_{12}(645\text{ nm}) \approx \sigma_T(645\text{ nm}) \approx 1.08 \times \sigma_{01}(645\text{ nm})$. These fits are depicted as solid lines in Fig. 6. Fits of comparable quality can be also obtained for intersystem crossing rates different from zero. Taking the very high value $k_{isc} = 1/(7\text{ ns})$ (≈66% of $1/\tau$ as for Chl a in solution), the best fit of the $\Phi_F(I_p)$ data is obtained with $\sigma_{01}(645\text{ nm}) = (1.15 \pm 0.1) \times 10^{-15}\text{ cm}^2$. In this case the fitting of $T(I_p)$ yields $k_{21} = 1/(250$ fs), and the relation $\sigma_{12}(645\text{ nm}) \approx \sigma_T(645\text{ nm}) \approx 1.08 \times \sigma_{01}(645\text{ nm})$ was the same as for $k_{isc} = 0$. These fits are depicted as dashed lines in Fig. 6.

Fig. 7 depicts the calculated relative populations of x_0, x_1, x_2, x_T and x_1^C (at the temporal maximum of the pulse) as a function of I_p for $k_{isc} = 1/(7\text{ ns})$. These data reveal that the depletion of the cluster ground state starts at relatively small

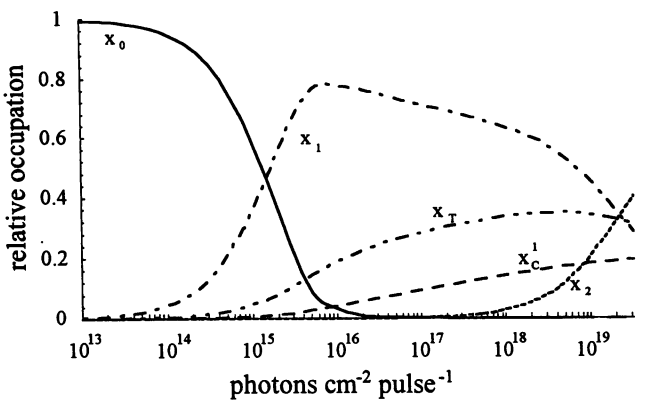

FIGURE 7 Calculated relative population of ground state and excited states according to the parameters from the dashed line of Fig. 6.

I_p values and is almost complete at $I_p \approx 10^{16}$ photons cm^{-2} $pulse^{-1}$, whereas the population of x_2 attains significant levels only at $I_p > 10^{18}$ photons cm^{-2} $pulse^{-1}$.

DISCUSSION

The most important result of this study is the finding that in the case of excitation with highly monochromatic ($\Delta\lambda \approx$ 0.002 nm) laser pulses of 2.5 ns duration and optimal spatial selectivity, the dependence of the normalized fluorescence yield, Φ_F, on the photon density, I_p, exhibits striking similarities with respect to the shape of the curves measured in solubilized LHCII and Chl a in dilute solution. The two curves are almost identical after a shift of the $\Phi_F(I_p)$ values of Chl a solutions by about 1.1 units in the logarithmic scale toward lower I_p. The Chl a data can be fitted accurately by a kinetic model for ground-state depletion, intersystem crossing, and relaxation (see Fits to the Data, above). This result obtained in dilute Chl a solution illustrates the quality of the experimental set-up.

The fluorescence data measured in solubilized LHCII can be described by a multiple hit model for an ensemble of pigment-protein subunits consisting of 10–15 chlorophylls. Within these subunits the fluorescence yield is assumed to be independent of the number κ of photons absorbed by this entity. This idea comprises a fast dissipative decay of multiple excitations within these subunits. The origin of this effect remains an open question. Therefore, a more elaborated kinetic model is proposed that takes into account strong pigment couplings within the subunits of LHCII. Within the framework of this model the excitons are considered as delocalized excited cluster states, and consequently the absorption of a second photon gives rise to an excited state absorption of the cluster rather than the formation of two excited states. Therefore, the concept of a bimolecular exciton-exciton annihilation in small units of strongly coupled pigments must be replaced by that of fast radiationless relaxation of higher delocalized cluster states. This idea implies questions on the domain size that is required to allow for the generation of double (S_1) excitations with accompanying singlet-singlet annihilation. However, the latter problem is beyond the scope of the present study and remains to be addressed by future investigations.

Based on the model of delocalized cluster states, data fitting was shown to be very successful. This analysis leads to two interesting conclusions: 1) The value σ_{01}(645 nm) exceeds the "chlorophyll monomer related" value by a factor of about 15 (for the case $k_{isc} = 1/(7\text{ ns})$). As a rough estimate this value represents the number of chlorophyll molecules constituting a delocalized cluster state (vide supra). 2) The relaxation of the second excited cluster state to the first excited cluster state takes place on a time scale of about 250 fs. As a consequence, the population x_2 significantly increases only at rather high I_p values (see Fig. 7).

The cluster model also provides a qualitative explanation for sub-picosecond two-color pump-probe experiments that were performed on the same type of solubilized LHCII as in the present study. Transient absorption changes were monitored at 655 nm and 680 nm after excitation of the samples with pump pulses at 645 nm and a duration of 130 fs (Bittner et al., 1994). The rise time of the 680-nm absorption changes of about 150 fs was interpreted as reflecting an ultrafast excitation energy transfer from Chl b to Chl a.

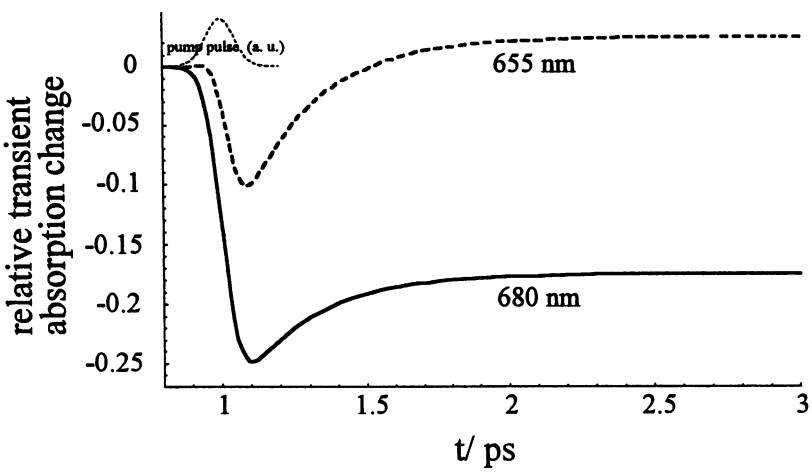

FIGURE 8 Calculated time course of relative transient absorption changes "tested" at 655 nm (– – –) and 680 nm (——) induced by a 130-fs pulse (at $t_0 = 1$ ps) with $I_p = 6 \cdot 10^{14}$ photons cm^{-2} $pulse^{-1}$ using the "pump" parameters gathered from data fitting in Fig. 6. The "test" parameters (see Appendix) were set as follows: $\sigma_{01}(655\text{ nm}) = 1.5 \cdot 10^{-15}$ cm^2, $\sigma_{01}(680\text{ nm}) = 2.2 \cdot 10^{-15}$ cm^2. $[\sigma_{12}(\lambda_{test}) - \sigma_{10}(\lambda_{test}) - \sigma_{01}(\lambda_{test})]/\sigma_{01}(\lambda_{test}) = 0.05$ for $\lambda_{test} = 655$ nm and -0.35 for $\lambda_{test} = 680$ nm, respectively.

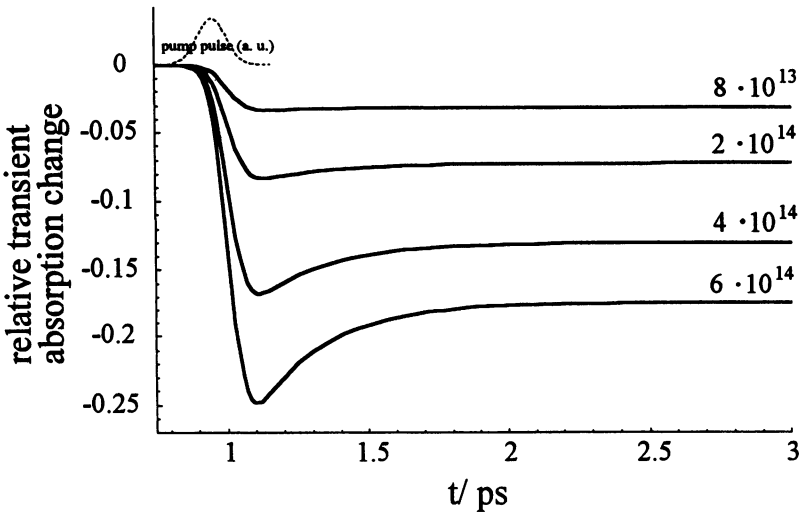

FIGURE 9 Time course of 680 nm relative transient absorption changes calculated for different photon densities (in photons cm^{-1} $pulse^{-1}$) of the 130-fs pump pulse at 645 nm. The parameters are the same as in Fig. 8.

However, if one takes into consideration that the 150-fs kinetics is probably limited by the time resolution of the equipment, the ultrafast rise at 680 nm could be alternatively interpreted within the cluster model as an "instantaneous" population of excited cluster states rather than as an ultrafast incoherent Förster-type excitation energy transfer from Chl b to Chl a. Recent theoretical calculations on the properties of excited cluster states in LHCII (Renger et al., 1996) support this idea. Likewise, the dependence of absorption changes on wavelength and excitation intensity reported in Bittner et al. (1994) can be qualitatively described. To illustrate this, the kinetics of the normalized populations $x_i(t, \lambda, I_p)$ with $i = 0, 1, 2$ were calculated (the formation of triplets is negligible at a picosecond time scale). Using the parameters gathered from the numerical fits of the relative fluorescence yield $\Phi_F(I_p)$ and the transmittance $T(I_p)$ (see Fig. 6), the time course of $\alpha(\lambda_{test}, t) - \alpha^0(\lambda_{test})$ was calculated as described in the Appendix. Fig. 8 depicts these curves obtained at $\lambda_{test} = 655$ nm and 680 nm under the assumption of a Gaussian pump pulse of 130 fs FWHM and a wavelength of 645 nm. Fig. 9 shows the calculated dependence of $\alpha(\lambda_{test}, t) - \alpha^0(\lambda_{test})$ at 680 nm on the photon density of the pump pulse. In both cases there is a close similarity to the experimental data reported by Bittner et al. (1994), clearly showing that the basic features of this ultrafast pump-probe experiment can be consistently explained by a model of delocalized states.

APPENDIX

The transient change of the absorption coefficient $\alpha(t) - \alpha^0$ is induced by a pump femtosecond pulse at 645 nm (at $t_0 = 1$ ps) and "tested" by a weak femtosecond pulse not affecting the excited-state populations. Because we consider a time scale of only a few picoseconds, the triplet formation is ineffective. In contrast to the pump pulses (at 645 nm), the test pulses at 655 nm and 680 nm can induce stimulated emission. Thus for the calculation of $\alpha(\lambda_{test}, t)$ the additional cross section $\sigma_{10}(\lambda_{test})$ for the stimulated emission must be considered. The (short time) transient absorption at λ_{test} results in

$$\alpha(\lambda_{test}, t) = N^{sample} \cdot \Big\{ \underbrace{\sigma_{01}(\lambda_{test}) \cdot [1 - x_1(t) - x_2(t)]}_{\text{ground state depletion}} \underbrace{- \sigma_{10}(\lambda_{test}) \cdot x_1(t)}_{\text{induced emission}} + \underbrace{\sigma_{12}(\lambda_{test}) \cdot x_1(t)}_{\text{excited state absorption}} \Big\}. \quad \text{(A1)}$$

Subtraction and subsequent division of the linear absorption coefficient lead to the relative transient absorption change:

$$\frac{\alpha(\lambda_{test}, t) - \alpha^0(\lambda_{test})}{\alpha^0(\lambda_{test})} = \underbrace{x_1(t) \cdot \left[\frac{\sigma_{12}(\lambda_{test}) - \sigma_{10}(\lambda_{test}) - \sigma_{01}(\lambda_{test})}{\sigma_{01}(\lambda_{test})} \right]}_{\text{"slow" term}} \underbrace{- x_2(t)}_{\text{"fast" term}}. \quad \text{(A2)}$$

$x_i(t)$ are known from the solution of Eqs. 3b–3f. Furthermore, it is easy to obtain the time derivatives of Eq. A2, because $d/dt\ x_i(t)$ follows directly from x_i and Eq. 3 itself.

For the calculation of $x_i(t)$ and $d/dt\ x_i(t)$, the parameters used were obtained from fitting of our experimental data (pump wavelength 645 nm), $\sigma_{01}(645\text{ nm}) = 1.15 \times 10^{-15}$ cm^2, $\sigma_{12}(645\text{ nm}) = 1.08 \times \sigma_{01}(645\text{ nm})$, $k_{10} = 1/(4.3\text{ ns})$, $k_{21} = 1/(0.25\text{ ps})$.

The ground-state absorption cross section σ_{01} at λ_{test} was calculated by

$$\sigma_{01}(\lambda_{test}) = \sigma_{01}(645\text{ nm}) \cdot \frac{OD(\lambda_{test})}{OD(645\text{ nm})}.$$

For $\lambda_{test} = 655$ nm and 680 nm, σ_{01} amounts to $\sigma_{01}(655\text{ nm}) = 1.5 \times 10^{-15}$ cm^2, $\sigma_{01}(680\text{ nm}) = 2.2 \times 10^{-15}$ cm^2.

To explain the experimental data of Bittner et al. (1994), the term

$$\frac{\sigma_{12}(\lambda_{test}) - \sigma_{10}(\lambda_{test}) - \sigma_{01}(\lambda_{test})}{\sigma_{01}(\lambda_{test})}$$

in Eq. A2 must be on the order of +0.05 at λ_{test} = 655 nm. At λ_{test} = 680 nm, σ_{01} and σ_{10} significantly exceed the value of σ_{12}, i.e.,

$$\frac{\sigma_{12}(\lambda_{test}) - \sigma_{10}(\lambda_{test}) - \sigma_{01}(\lambda_{test})}{\sigma_{01}(\lambda_{test})}$$

is negative. For the calculation of the curve this expression was set at −0.35. In accordance with the experimental data of Bittner et al. (1994), this gives rise to a "long time" decrease of

$$\frac{\alpha(\lambda_{test}, t) - \alpha^0(\lambda_{test})}{\alpha^0(\lambda_{test})}$$

(see Fig. 8).

The financial support by Deutsche Forschungsgemeinschaft (Sfb 312) is gratefully acknowledged.

REFERENCES

Beddard, G. S., G. Porter, C. J. Tredwell, and J. Barber. 1975. Fluorescence lifetimes in the photosynthetic unit. *Nature.* 258:166–168.

Berthold, D. A., G. T. Babcock, and C. F. Yocum. 1981. A highly resolved, oxygen-evolving photosystem II preparation from spinach thylakoid membranes. *FEBS Lett.* 134:231–234.

Bittner, T., K.-D. Irrgang, G. Renger, and M. R. Wasilewski. 1994. Ultrafast excitation energy transfer and exciton-exciton annihilation processes in isolated light harvesting complexes of photosystem II (LHC II) from spinach. *J. Phys. Chem.* 98:11821–11826.

Bowers, P. G., and G. Porter. 1967. Quantum yields of triplet formation in solutions of chlorophyll. *Proc. R. Soc. London.* A296:435–441.

Breton, J., and N. E. Geacintov. 1976. Quenching of fluorescence of chlorophyll in vivo by long-lived excited states. *FEBS Lett.* 69:86–89.

Breton, J., and N. E. Geacintov. 1980. Picosecond fluorescence kinetics and fast energy transfer processes in photosynthetic membranes. *Biochim. Biophys. Acta.* 594:1–32.

Campillo, A. J., V.-H. Kollman, and S. L. Shapiro. 1976a. Intensity dependence of the fluorescence lifetime in vivo chlorophyll excited by a picosecond light pulse. *Science.* 193:227–229.

Campillo, A. J., S. L. Shapiro, V.-H. Kollman, K. R. Winn, and R. C. Hyer. 1976b. Picosecond excitation annihilation in photosynthetic systems. *Biophys. J.* 16:93–97.

Förster, Th. 1948. Zwischenmolekulare Energiewanderung und Fluoreszenz. *Ann. Phys.* 6:55–75.

Geacintov, N. E., J. Breton, C. E. Swenberg, A. J. Campillo, S. L. Shapiro, and R. C. Hyer. 1977a. Picosecond and microsecond pulse laser studies of excitation quenching and excitation distribution in spinach chloroplasts at low temperatures. *Biochim. Biophys. Acta.* 461:306–312.

Geacintov, N. E., J. Breton, C. E. Swenberg, and G. Paillotin. 1977b. A single pulse picosecond laser study of exciton dynamics in chloroplasts. *Photochem. Photobiol.* 26:629–638.

Geacintov, N. E., D. Husiak, T. Kolubayev, J. Breton, A. J. Campillo, S. L. Shapiro, K. R. Winn, and P. K. Woodbridge. 1979. Exciton annihilation versus excited state absorption and stimulated emission effects in laser studies of fluorescence quenching of chlorophyll in vitro and in vivo. *Chem. Phys. Lett.* 66:154–158.

Geacintov, N. E., C. E. Swenberg, A. J. Campillo, R. C. Hyer, S. L. Shapiro, and K. R. Winn. 1978. A picosecond pulse train study of exciton dynamics in photosynthetic membranes. *Biophys. J.* 24: 347–359.

Gülen, D., B. P. Wittmershaus, and R. S. Knox. 1986. Theory of picosecond-laser-induced fluorescence from highly excited complexes with small numbers of chromophores. *Biophys. J.* 49:469–477.

Holzwarth, A. R. 1989. Applications of ultrafast laser spectroscopy for the study of biological systems. *Q. Rev. Biophys.* 22:239–295.

Irrgang, K.-D., E. J. Boekema, J. Vater, and G. Renger. 1988. Structural determination of the photosystem II core complex from spinach. *Eur. J. Biochem.* 178:209–217.

Jansson, S. 1994. The light-harvesting chlorophyll a/b-binding proteins. *Biochim. Biophys. Acta.* 1184:1–19.

Kolubajev, T., N. E. Geacintov, G. Paillotin, and J. Breton. 1985. Domain sizes in chloroplasts and chlorophyll-protein complexes probed by fluorescence yield quenching induced by singlet-triplet exciton annihilation. *Biochim. Biophys. Acta.* 808:66–76.

Kramer, H., and P. Mathis. 1980. Quantum yield and rate of formation of the carotenoid triplet state in photosynthetic structures. *Biochim. Biophys. Acta.* 593:319–329.

Kühlbrandt, W. 1994. Structure and function of the plant light-harvesting complex, LHCII. *Curr. Biol.* 4:519–528.

Kühlbrandt, W., D. N. Wang, and Y. Fujiyoshi. 1994. Atomic model of plant light-harvesting complex by electron crystallography. *Nature.* 367: 614–621.

Kwa, S. L. S., F. G. Groeneveld, J. P. Dekker, R. van Grondelle, H. van Amerongen, S. Lin, and W. S. Struve. 1992. Steady-state and time-resolved polarized light spectroscopy of the green plant light-harvesting complex II. *Biochim. Biophys. Acta.* 1101:143–146.

Liu, B., A. Napiwotzki, H.-J. Eckert, H. J. Eichler, and G. Renger. 1993. Studies on the recombination kinetics of the radical pair $P680^+Pheo^-$ in isolated PS II core complexes from spinach. *Biochim. Biophys. Acta.* 1142:129–138.

Mauzerall, D. 1976a. Multiple excitations in photosynthetic systems. *Biophys. J.* 16:87–91.

Mauzerall, D. 1976b. Fluorescence and multiple excitation in photosynthetic systems. *J. Phys. Chem.* 80:2306–2309.

Mauzerall, D. 1978. Multiple excitations and the yield of chlorophyll a fluorescence in photosynthetic systems. *Photochem. Photobiol.* 28: 991–998.

Mukamel, S. 1995. Signatures of cooperativity: two exciton resonances and enhanced nonlinear susceptibilities in molecular aggregates. *In* Principles of Nonlinear Optical Spectroscopy. Oxford University Press, Oxford. 498–507.

Mukamel, S., and V. Rupasov. 1995. Energy transfer, spectral diffusion, and fluorescence of molecular aggregates: Brownian oscillator analysis. *Chem. Phys. Lett.* 242:17–26.

Nordlund, T. M., and W. H. Knox. 1981. Lifetime of fluorescence from light harvesting chlorophyll a/b proteins excitation intensity dependence. *Biophys. J.* 38:193–201.

Nussberger, S., J. P. Dekker, W. Kühlbrandt, B. M. van Bolhuis, R. van Grondelle, and H. van Amerongen. 1994. Spectroscopic characterization of three different monomeric forms of the main chlorophyll a/b binding from chloroplast membranes. *Biochemistry.* 33:14775–14783.

Paillotin, G., N. E. Geacintov, and J. Breton. 1983a. A master equation theory of fluorescence induction, photochemical yield, and singlet-triplet exciton quenching in photosynthetic systems. *Biophys. J.* 44:65–77.

Paillotin, G., N. E. Geacintov, and J. Breton. 1983b. Effect of spatial non-uniformity of illumination in non-linear intensity dependent photophysical experiments. Application to some fluorescence yield measurements in photosynthetic systems. *Photochem. Photobiol.* 37:475–478.

Paillotin, G., C. E. Swenberg, J. Breton, and N. E. Geacintov. 1979. Analysis of picosecond laser-induced fluorescence phenomena in photosynthetic membranes utilizing a master equation approach. *Biophys. J.* 25:513–534.

Paschenko, V. Z., S. P. Protasov, A. B. Rubin, K. N. Timofeev, L. M. Zamazova, and L. B. Rubin. 1975. Probing the kinetics of photosystem I and photosystem II fluorescence in pea cloroplasts on a picosecond pulse fluorimeter. *Biochim. Biophys. Acta.* 408:143–153.

Paulsen, H. 1995. Chlorophyll a/b binding proteins. *Photochem. Photobiol.* 62:367–382.

Petermann, E. J. G., F. M. Dukker, R. van Grondelle, and H. van Amerongen. 1995. Chlorophyll a and carotenoid states in light harvesting complex II of higher plants. *Biophys. J.* 69:2670–2678.

Porra, R. J., W. A. Thompson, and P. E. Kriedemann. 1989. Determination of accurate extinction coefficients and simultaneous equations for assaying chl a and b extracted with for different solvents: verification of the concentration of chl standards by atomic absorption spectroscopy. *Biochim. Biophys. Acta.* 975:384–394.

Pulles, M. P. J., H. J. van Gorkom, and G. A. M. Verschoor. 1976. Primary reactions of photosystem II at low pH 2. Light induced changes of absorbance and electron spin resonance in spinach chloroplasts. *Biochim. Biophys. Acta.* 440:98–106.

Renger, G. 1992. Energy transfer and trapping in photosystem II. *In* Topics in Photosynthesis, Vol. 11. J. Barber, editor. Elsevier, Amsterdam. 45–99.

Renger, G., and U. Schreiber. 1986. Practical application of fluorometric methods to algae and higher plant research. D. C. Fork, Govindjee, and J. Amesz, editors. Academic Press, New York. 587–619.

Renger, T., J. Voigt, and V. May 1996. Theory of ultrafast pump-probe spectra: dissipative exciton motion in the light-harvesting complex of photosystem II. *J. Phys. Chem.* 39:15654.

Rubin, L. B., and V. Z. Paschenko. 1986. Electron excitation energy distribution in the photosynthetic pigment apparatus of green plants. *Lasers Life Sci.* 1:171–192.

Schödel, R., J. Voigt, and G. Kehrberg. 1994. Non-linar fluorescence yield of photosystem 2 subunits of higher plants. *Photosynthetica.* 30:613–622.

Seibert, M., and R. R. Alfons. 1974. Probing photosynthesis on a picosecond time scale. *Biophys. J.* 14:269–283.

Siefermann-Harms, D. 1987. The light harvesting protective functions of carotenoids in photosynthetic membranes. *Physiol. Plantarum.* 69: 561–568.

Swenberg, C. E., N. E. Geacintov, and M. Pope. 1976. Bimolecular quenching of excitons and fluorescence in the photosynthetic unit. *Biophys. J.* 16:1447–1452.

Thornber, J. P., R. J. Cogdell, P. Chitnis, D. T. Morishige, G. F. Peter, S. M. Gomez, S. Anandan, S. Preiss, B. W. Dreyfuss, A. Lee, T. Takeuchi, and C. Kerfeld. 1994. Antenna pigment-protein complexes of higher plants and purple bacteria. *Adv. Mol. Cell. Biol.* 10:55–118.

Valkunas, L., G. Trinkunas, V. Liuolia, and R. Van Grondelle. 1995. Nonlinear annihilation of excitations in photosynthetic systems. *Biophys. J.* 69:1117–1129.

Van Grondelle, R., J. P. Dekker, T. Gillbro, and V. Sundstrom. 1994. Energy transfer and trapping in photosynthesis. *Biochim. Biophys. Acta.* 1187:1–65.

Vasilev, S., T. Schrötter, A. Bergmann, K.-D. Irrgang, H. J. Eichler, and G. Renger. 1996. Cryoprotectant induced quenching of chlorophyll a fluorescence from LHCII in vitro: time resolved and study state spectroscopic studies. *Photosynthetica.* In press.

Völker, M., T. A. Ono, Y. Inoue, and G. Renger. 1985. Effect of trypsin on PS II particles. Correlation between Hill activity, Mn abundance and peptide pattern. *Biochim. Biophys. Acta.* 806:25–34.